Meteorologische Zeitschrift, Vol. **19**, No. 5, 453-466 (October 2010)

Article

The case study of bura of 1st and 3rd February 2007

MARTINA TUDOR* and STJEPAN IVATEK-ŠAHDAN

[1]Croatian meteorological and hydrological service, Croatia

(Manuscript received October 10, 2009; in revised form July 16, 2010; accepted August 18, 2010)

Abstract

Two cases when the operational forecast seriously underestimated the wind speed maxima are analysed. The first one in the night between 1st and 2nd February 2007 and the second one in the evening of 3rd February 2007. The two cases are analyzed using measured data from Split and Makarska automatic stations as well as vertical soundings from Zagreb and Zadar and ALADIN model simulations. For the purpose of this study, ALADIN 72 hour forecast was run on 2 km resolution using the complete set of physics parametrizations, hydrostatic and nonhydrostatic dynamics. Results show the potential benefit of nonhydrostatic dynamics for operational forecast does not lie in improvement of the 10 m wind forecast as much as in forecasting clear air turbulence associated with the lee waves.

Zusammenfassung

Es werden zwei Wetterlagen, in denen die operationelle Vorhersage die maximalen Geschwindigkeiten der Bora an der kroatischen Küste unterschätzt hat, untersucht. Die erste ereignete sich in der Nacht vom 1. zum 2. Februar 2007, die andere am Abend des 3. Februar 2007. Zur Untersuchung werden die Messdaten von den automatischen Stationen in Split und Makarska sowie die Radiosondenaufstiege von Zagreb und Simulationen mit dem Modell ALADIN benutzt. Mit dem Modell ALADIN werden 72 Stunden-Vorhersagen mit 2 km Auflösung unter Benutzung des kompletten Satzes physikalischer Parametrisierungen mit hydrostatischer und nicht-hydrostatischer Dynamik gerechnet. Die Ergebnisse zeigen, dass der potentielle Nutzen der nichthydrostatischen Dynamik für die operationelle Vorhersage nicht so sehr in der Verbesserung der 10 m Windvorhersage liegt, sondern vielmehr in der Vorhersage der mit den Leewellen verbundenen "clear air turbulence".

1 Introduction

This article has been inspired by the failure of the operational forecast model to predict the two cases of bura (the Croatian expression for bora) at the beginning of February 2007. The operational high-resolution forecast of the 10 m wind in the cases of strong to severe bura wind, using the dynamical adaptation method adapted from ŽAGAR and RAKOVEC (1999), and using the hydrostatic version of the ALADIN model, has been considered successfull so far (IVATEK-ŠAHDAN and TUDOR, 2004). This encouraged the use of the same method to estimate the expected extreme wind speeds in different locations and for different purposes (eg. TUDOR and IVATEK-ŠAHDAN, 2002; BAJIĆ et al., 2007).

GRISOGONO and BELUŠIĆ (2009) give a comprehensive review of recent advances in bura research. The numerous theories of bura development were tested on the ALPEX field experiment data (SMITH, 1987) by DURRAN (1986a) who applied the wave breaking theory (PELTIER and CLARK, 1979) and the hydraulic theory (SMITH, 1985) to several cases. The hydraulic theory was further investigated using a numerical model in KLEMP and DURRAN (1987).

The case studies of bura wind in Croatia are numerous (eg. BRZOVIĆ, 1999a; JURČEC and BRZOVIĆ, 1995). The studies using numerical weather prediction (NWP) models are fewer, and these are limited to particular cases (eg. BRZOVIĆ and JURČEC, 1997 and HORVATH et al., 2009) with few sensitivity studies (eg. BRZOVIĆ, 1999b; ENGER and GRISOGONO, 1998 and IVATEK-ŠAHDAN and IVANČAN-PICEK, 2006).

Downslope windstorms are transient phenomena. The flow over the topography becomes unsteady and the internal waves generated by topography become locally convectively unstable (CLARK and PELTIER, 1977). Stratified flow over an obstacle generates nonlinear waves that are found linearly unstable (LAPRISE and PELTIER, 1989b) and lead to intense downslope windstorms. The unstable modes of nonlinear mountain waves, for the Froude number exceeding a critical value, are found when the vertically propagating wave steepens until streamlines overturn causing local reversal of the flow and a superadiabatic region. This solution is refered to as local convective mode in LAPRISE and PELTIER (1989b) and is found temporally episodic (LAPRISE and PELTIER, 1989a). The vertically propagating wave energy is trapped between the region of maximum wave steepness and the surface. This energy produces the deep resonant mode (LAPRISE and PELTIER, 1989c) that is responsible for the transition from vertically propagating wave to downslope windstorm. The region of overturning streamlines has Richardson number lower than critical value and supports generation of turbulent ki-

*Corresponding author: Martina Tudor, Croatian meteorological and hydrological service, Grič 3, 10000 Zagreb, Croatia, e-mail: tudor@cirus.dhz.hr

DOI 10.1127/0941-2948/2010/0475

0941-2948/2010/0475 $ 6.30

netic energy that feeds the deep resonant mode that in turn accelerates the low level flow in the lee of the obstacle (LAPRISE and PELTIER, 1989a).

Both hydrostatic and nonhydrostatic nonlinear waves have larger amplitude than the one predicted by the linear theory (PELTIER and CLARK, 1979). The nonlinear effects are those that lead to wave breaking, but the associated convective instability in the region of overturning streamlines is expected to be present only in the nonhydrostatic model (PELTIER and CLARK, 1979). Wave steepening, breaking and overturning leads to formation of a turbulent region aloft that can partially reflect vertically propagating waves and increase the intensity of the downslope windstorm (SMITH, 1979; KLEMP and DURRAN, 1987; CLARK and PELTIER, 1977). Nondispersive vertically propagating waves are generated by buoyancy dominated hydrostatic flow, while the waves that trail downstream behind a vertically propagating dispersive wave reveal significant influence of nonhydrostatic effects (SMITH, 1979). The two-dimensional analyses showed that additional waves appear downstream of the mountain only if nonhydrostatic effects are important (DURRAN, 1986b). However, an isolated mountain in three dimensions can generate hydrostatic waves downstream and to the side of the mountain (SMITH, 1979).

Hydrostatic assumption eliminates trapped or partially trapped waves propagating downstream. Solutions for mountain waves with and without the hydrostatic assumption for linearized steady state equations for the atmosphere with constant wind and stability were derived by QUENEY (1948). These results encouraged the use of the hydrostatic assumption for broad mountains. This assumption was questioned by KELLER (1994) who showed the non-hydrostatic trapping effect of the wind shear and that the broad but irregular obstacle can generate substantial non-hydrostatic modes. Nonhydrostatic effects are less important for extreme large amplitude waves (KELLER, 1994). LAPRISE and PELTIER (1989a) compare nonhydrostatic and hydrostatic nonlinear solutions and find that overturning of streamlines in the nonhydrostatic solution requires higher obstacle, happens further downstream and at a lower height.

The Scorer parameter is used to distinguish the importance of nonhydrostatic effects. It is usually defined as $l^2 = \frac{N^2}{U^2} - \frac{1}{u}\frac{\partial^2 U}{\partial z^2}$ where N is The Brunt Vaisala frequency and u the wind component perpendicular to the mountain. The second term is sometimes neglected, but the wind shear contribution can be important (KELLER, 1994) in supporting nonhydrostatic effects. It is assumed that the flow is hydrostatic if $al \ll 1$ and nonhydrostatic for $al \sim 1$ where a is the halfwidth of the mountain. It is assumed that linear approximation is valid for problems where $\frac{Nh}{u} \ll 1$, while nonlinear effects become important if $\frac{Nh}{u} \sim 1$, where h is the mountain height.

Simulations of WANG and LIN (2000) show that the Boulder windstorm does not happen if the near mountain top inversion is missing or moved higher, but a less stable layer below the tropopause supports the windstorm development even without the inversion.

Strong stable layer in the lower atmosphere and/or increase in cross-mountain component of wind with height induce trapped lee waves (SMITH, 1979) that interfere with other mountains downstream. The presence of the second obstacle promotes wave trapping and modulates the wave amplitude (GRUBIŠIĆ and STIPERSKI, 2009). High amplitude mountain waves have been linked with the formation of rotors downstream. Two types of rotor systems are distinguished (HERTENSTEIN and KUETTNER, 2005). The first one is associated with the trapped lee waves. The second type resembles a hydraulic jump. Small vertical shear, strong stability, high and steep lee slopes, all favor hydraulic jump rotors that are usually more turbulent (HERTENSTEIN, 2009).

The horizontal wavelength of the trapped lee waves increases with the deepening of the mixed layer, which thins the stable inversion layer (RALPH et al., 1997). The irregular variations in the wavelength of the trapped lee waves are a consequence of temporal evolution of background flow (NANCE and DURRAN, 1998) or, more likely, generated by nonlinear wave dynamics (NANCE and DURRAN, 1997).

Several cases of rather short but intensive bura wind were not forecast in Croatian Meteorological and Hydrological Service (CMHS) by the operational dynamical adaptation using a hydrostatic model. The operational set-up of the high-resolution dynamical adaptation is hydrostatic, run on reduced number of levels in the vertical and neglects considerable number of physical processes (IVATEK-ŠAHDAN and TUDOR, 2004). Although the unpredicted bura episodes lasted only for several hours, their strength was sufficient to produce enough damage to the objects and disturb local traffic that the failure to predict them is a serious issue. The purpose of this study is to investigate if nonhydrostatic effects produce the short bura episodes.

The bura episodes studied here are rather short and connected with a pressure disturbance, therefore the study focuses on two points on the Croatian coast hit by these bura episodes (Split and Makarska) where the automatic 10-minute measurements of 10 meter wind and pressure are available. The two points are characterized by different terrain configuration upstream with various local mechanisms affecting the onset, duration and strength of the bura wind (Figure 1). The Dinaric Alps upstream of Split and Makarska are wide, but consist of many ridges separated by valleys and gaps.

The particular two episodes analyzed in this article were chosen since both of them hit the same areas most severely and both can be covered by a single 72 hour forecast run. Other forecast runs, starting from different analyses, did not perform any better, in forecasting the wind speed, in the area hit by the strong to severe bura episodes.

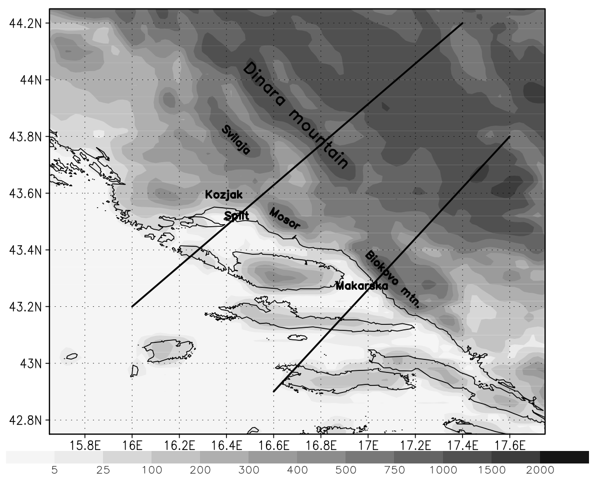

Figure 1: Terrain height in 2 km resolution. Split and Makarska are locations where the measurements from the automatic stations are taken. The vertical cross-sections are shown as full lines.

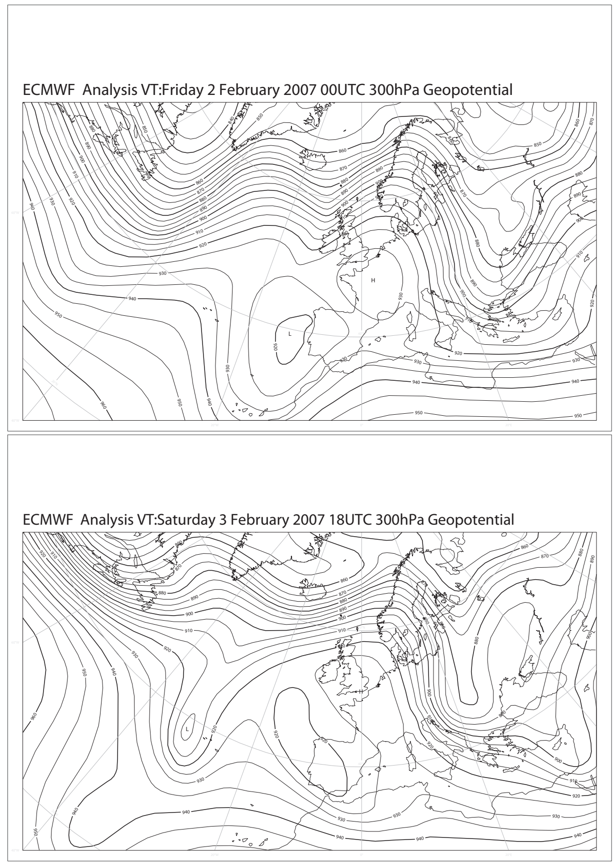

Figure 2: ECMWF analysis of 300 hPa geopotential for 2nd February 2007 00 UTC (top) and 3rd February 2007 18 UTC (bottom).

One of the reviewers remarked that the short lived bura events are too sensitive to the initial conditions to be predictable. REINECKE and DURRAN (2009) studied the predictability of similar downslope windstorms on two cases in the Owens Valley and found large differences in the predicted wind speed for the upstream conditions that varied less than the radiosonde observation errors. This result diminishes the hope that improvements in the data assimilation (eg. done in higher resolution with more measurements) might improve the results of the operational model forecast. However, several studies are more encouraging. IVATEK-ŠAHDAN and IVANČAN-PICEK (2006) find little importance of the different initial conditions for the MAP-IOP15 wind storm case. HORVATH et al. (2009) suggests that the numerical prediction of the southern bura events is less affected by the small uncertainties in the upstream conditions.

Proper assesment of the predictability of such short but severe episodes of bura requires an excersize similar to the work done in BRANKOVIĆ et al. (2008) but for the cases of short severe bura. The predictability of one case of severe bura (BRANKOVIĆ et al., 2007) showed that the gale force bura in the northern Adriatic was predicted with probability exceeding 95 % but with less success further south.

The next section briefly describes the synoptic situation during the bura episodes. Third section describes the ALADIN model set-up used in this study. Results of model simulations are presented in Section 4. The last section brings conclusions.

2 Synoptic situation and wind measurements

On 1st February 2007, there is an upper level through moving southeastward from the Baltic to the Black sea (Figure 2a). Associated with this through, there is a northwest jet stream in the middle and upper troposphere over Central Europe. As the center moves southward, high level wind above the eastern Adriatic coast changes the direction from northwest to north and later northeast. Wind is first parallel to the mountains close to the coastline, and later almost perpendicular to them. The jet moves further south on 2nd February 2007 only to be replaced by another northwest jet that is part of another upper level through that formed over the Baltic sea and spread south to the Balkan peninsula. On 3rd February 2007 the air flow in the middle and upper troposphere is parallel to the mountains (Figure 2b). It first strengthens without significant changes in the direction. After 18 UTC the wind changes the direction, it is first north and later northeast, increasing the wind component perpendicular to the mountains. Lower in the troposphere, at the 850 hPa level, close to the mountain top height, wind speed is much lower, but the larger portion of it belongs to the component perpendicular to the mountains.

Measurements are taken from the two automatic stations situated in Split and Makarska that measure 10 m wind speed and direction as well as pressure. The stations are characterized by different terrain configuration

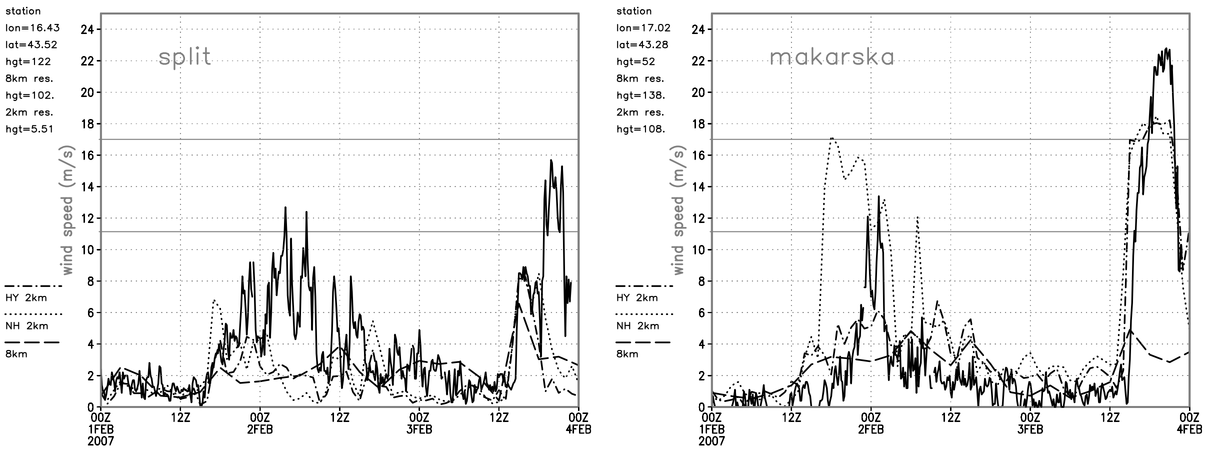

Figure 3: 10 minute measurements (full line) of wind speed 10 meters above ground, the 72 hour forecast runs starting from 00 UTC 1st February 2007 in 8 km resolution (dashed line), 2 km resolution full run with hydrostatic (dot dash line) and non-hydrostatic (dotted line) dynamics for Split (a) and Makarska (b) locations. The longitude and latitude of the measuring station locations as well as height above the sea level are also shown.

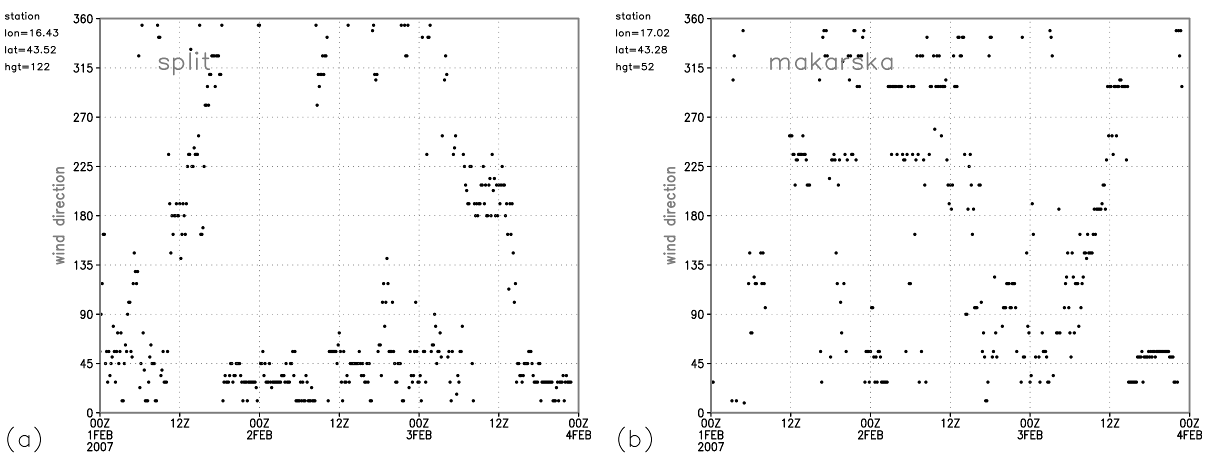

Figure 4: 10 minute measurements (full circle) of wind direction 10 meters above ground. for Split (a) and Makarska (b) locations. The longitude and latitude of the measuring station locations as well as height above the sea level are also shown. wind direction.

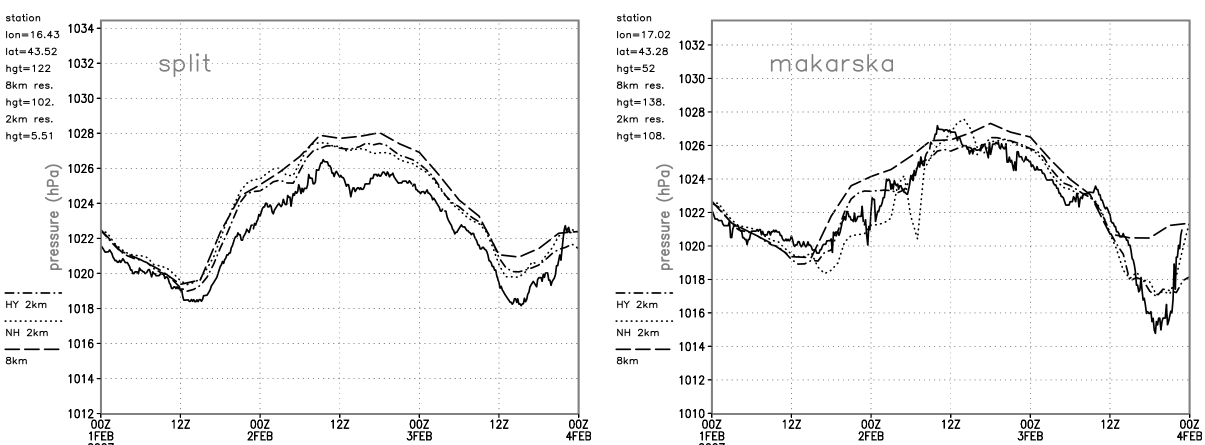

Figure 5: As Figure 3 but for pressure reduced to mean sea level.

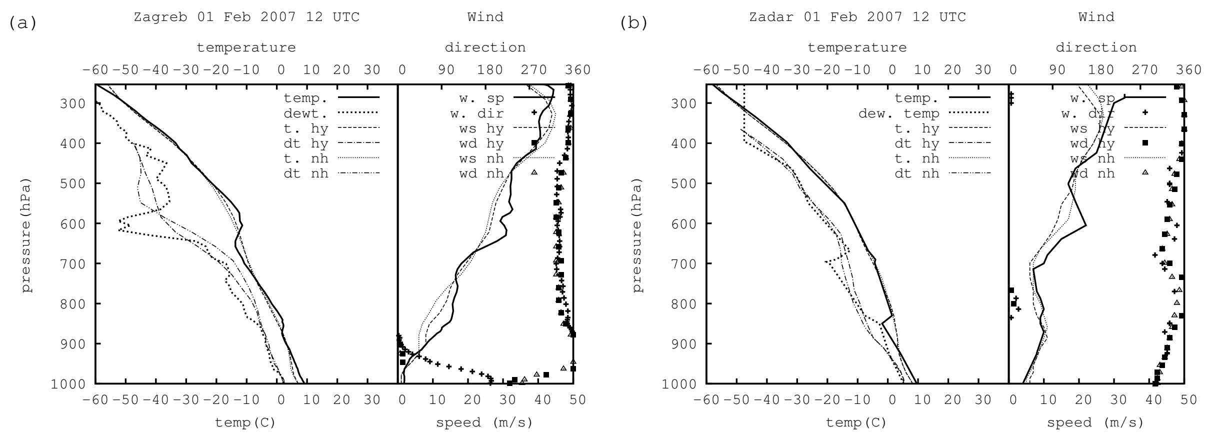

Figure 6: Measured and forecast vertical profiles of temperature and wind for Zagreb (left) and Zadar (right) locations for 12 UTC on 1st February 2007. The left frames present measured temperature (full line), dewpoint temperature (thick dotted line), modelled temperature (dashed) and dewpoint temperature (dot dash) using hydrostatic dynamics and modelled temperature (thin dotted) and dewpoint temperature (dot dot dash) using nonhydrostatic dynamics. Right frames present measured wind speed (full line) and direction (plus sign), modelled wind speed (dashed) and direction (square) using hydrostatic dynamics and modelled wind speed (thin dotted) and direction (triangle) using nonhydrostatic dynamics.

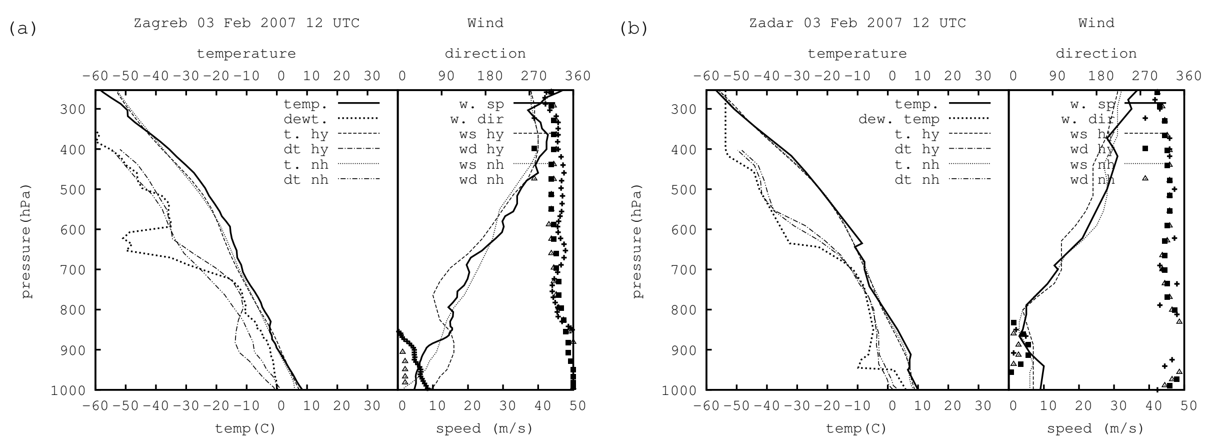

Figure 7: As Figure 6 but for 12 UTC on 3rd February 2007.

upstream. The Split station is situated southwest of a mountain pass (downstream of the mountain pass in bura episodes) and the Makarska station has Biokovo mountain ridge to the northeast (upstream in bura episodes) (Figure 1).

During the evening of 1st and and the night of 2nd February 2007, the 10 m wind speed measured on the automatic stations in Split and Makarska significantly exceeded the forecast one (Figure 3). Average 10 minute wind rapidly changed between mild to strong and back, from one interval to the next, but remained northeast during both severe wind episodes (Figure 4). Simultaneously, the pressure also showed rapid oscillations with a 1 hPa amplitude superimposed on increasing pressure trend (Figure 5). The pressure increased for 8 hPa during 20 hours, starting from 14 UTC on 1st February 2007 until 10 UTC the next day. During the same period, wind speed in Split varied rapidly with an amplitude increasing with time, around the mean wind speed that also increased, while the wind direction varied between northeast and north. In Makarska, there were two outbursts of strong bura, both lasting for about an hour, during an otherwise calm night. Simultaneosly with both peaks in the wind speed, associated strong decrease in pressure can be observed. The variations in the pressure field were much stronger in Makarska than in Split.

Vertical sounding data were taken from two Croatian measuring stations. Zagreb station is situated in a valley in inland Croatia, upstream of the coastal mountains and far from the region hit most severely by this bura episode, about 250 km north of Split. Zadar station is located on the eastern Adriatic coast, downstream of the mountains about 120 km northwest of Split. Vertical sounding data (Figure 6a) from Zagreb station for 12 UTC 1st February 2007 show two temperature inversions, at 850 and at 650 hPa, with low wind speed at the surface, weak wind shear in the inversion layers and strong shear layers below and above the stable layers. The wind shear is strong due to rapid increase of wind speed with height since the wind direction remains

NNW above the slow layer close to surface. Measured vertical profiles at Zadar station show one temperature inversion at 850 hPa with strong surface wind, weak shear in the layer below the inversion and a stronger shear above (Figure 6b). Wind speed is lower for Zadar than for Zagreb throughout the troposphere, except in the lowest 1 km.

The second bura episode, in the evening of 3rd February 2007 was characterized by much stronger and more steady NE wind (Figure 3) associated with a rapid decrease in pressure that was much stronger in Makarska (8 hPa) than in Split (4 hPa) (Figure 5). There were two stable layers above Zagreb, at 850 and 600 hPa, not associated with temperature inversion but more stable than adjacent layers in the vertical. Wind speed increased with height up to 7 km (Figure 7a). The stable layers above Zadar are stronger, with temperature inversions at 975 and 650 hPa (Figure 7b). Surface wind speed is much stronger and decreases with height in the lower inversion layer. Above it, wind shear is strong due to rapid increase of wind speed with height in the layer between the two temperature inversions. Again, the wind is stronger above Zagreb at all heights above 1 km, and in Zadar below 1 km.

The wind direction of about 45 degrees would be perpendicular to the coastal mountains, however both soundings are not directly upstream nor downstream of the area shown. The Zagreb sounding could be representative for upstream conditions for the whole Dinaric Alps range. The sounding upstream of the last ridge could be significantly different. Wide southern Dinaric Alps contain many ridges of variable height, width and orientation so that the cross mountain component cannot be defined in a unique way.

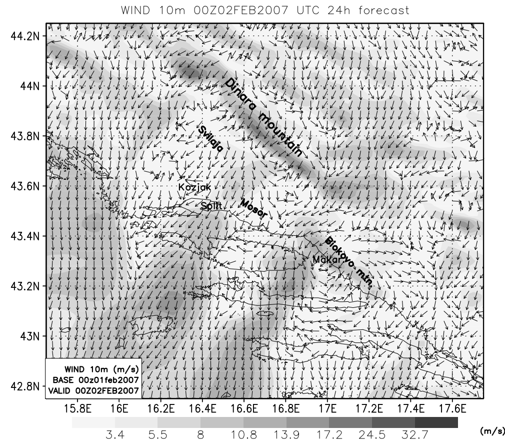

Figure 8: Forecast of wind 10 m above ground speed (shaded) and direction (vectors) for 00 UTC 2nd February 2007.

3 Model setup

The operational forecast is performed using the hydrostatic version of ALADIN (Aire Limitée Adaptation Dynamique dévelopement InterNational) model with 8 km horizontal resolution on 37 levels in the vertical. It is a spectral model that uses double Fourier representation of fields with elliptic truncation (MACHENHAUER and HAUGEN, 1987) and a hybrid pressure-type terrain-following η coordinate (SIMMONS and BURRIDGE, 1981). Operationally, the 8 km resolution run is initialized using digital filter initialization (DFI) (LYNCH and HUANG, 1994). The model version used operationally in 2007 has changed from the one described in IVATEK-ŠAHDAN and TUDOR (2004). The primitive equation set for the wind components, temperature, specific humidity, cloud water and ice, rain and snow as well as surface pressure is solved using the two-time-level semi-implicit semi-lagrangian integration scheme.

There are two horizontal diffusion schemes in ALADIN model. One is a common 4th order numerical horizontal diffusion (NHD) scheme that acts as a numerical filter and selectively dampens the short waves. NHD is applied on model levels in spectral space. Since model levels follow orography, NHD is not purely horizontal. NHD is not physical since it depends on the model geometry and not on the state of the atmosphere nor on the flow properties. The semi-lagrangian horizontal diffusion (SLHD) is a horizontal diffusion scheme based on the physical properties of the flow (VÁŇA et al., 2008). SLHD scheme is more dependant on the state of the atmosphere and flow properties and is therefore more physical. When both schemes are activated, the intensity of NHD is significantly reduced.

The part of the model that changed more significantly is the physical parameterization package. The vertical diffusion parameterization has been upgraded from LOUIS et al. (1982) to include effects of prognostic turbulent kinetic energy (TKE) scheme (GELEYN et al., 2006) extending to the whole atmosphere the work of REDELSPERGER et al. (2001) who matched the full TKE sub-grid scale scheme and similarity laws in the surface layer. The turbulent exchange coefficients are now computed using the TKE, which is now a prognostic model variable. A simple microphysics scheme for prognostic cloud water and ice, rain and snow (CATRY et al., 2007) with statistical sedimentation (GELEYN et al., 2008) has been introduced as well.

The 8 km resolution forecast is operationally further dynamically downscaled to 2 km horizontal resolution on a single domain of 450x450 points, using the same procedure as described in IVATEK-ŠAHDAN and TUDOR (2004). Instead of running the full model forecast on 2 km resolution for 72 hours, each output file of 8 km resolution is used as initial and coupling file and the forecast is run on only 15 levels using hydrostatic dynamics and vertical turbulent diffusion parameterization. The model is run for 30 one-minute timesteps which allows wind to adapt dynamically to the high resolution terrain representation. This operational forecast failed to predict the severe bura episodes so the results of more demanding model runs are presented here.

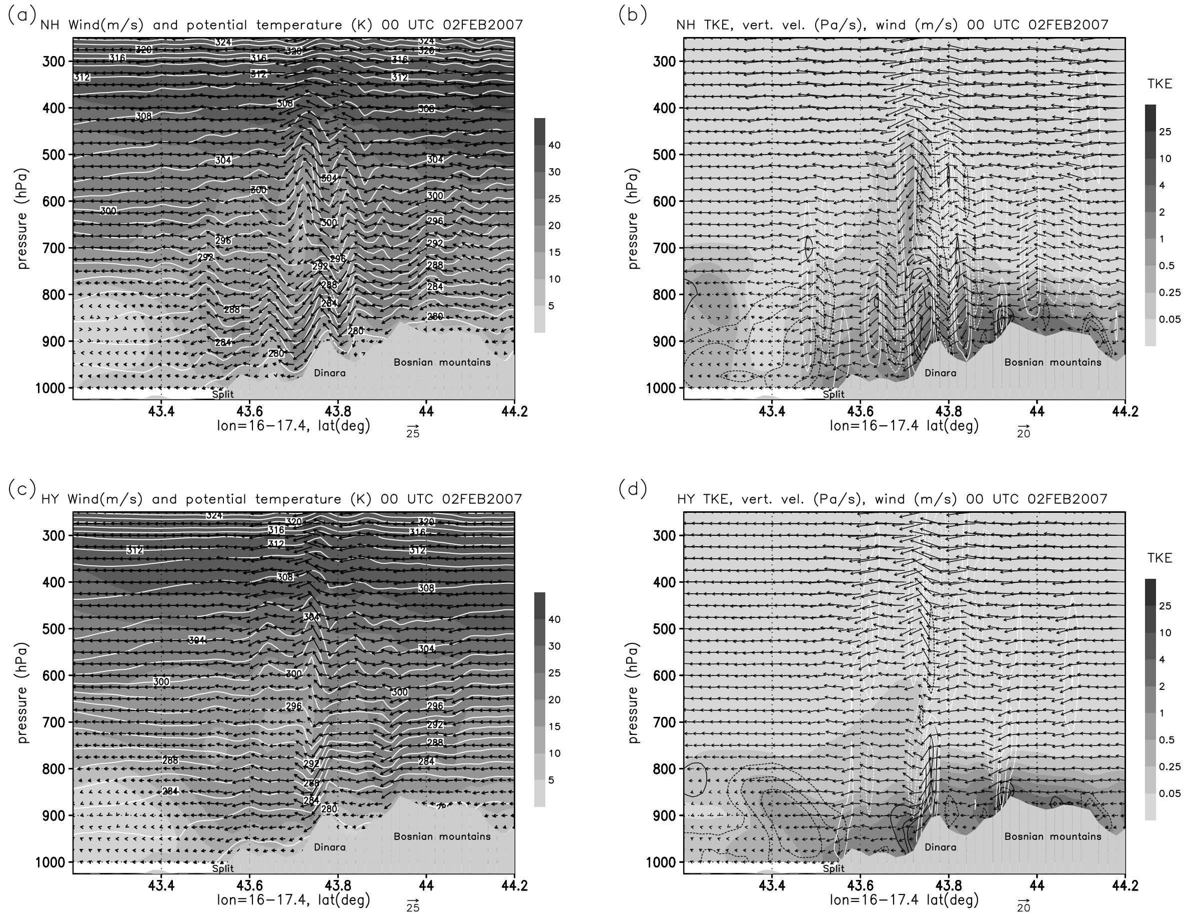

Figure 9: Vertical cross-sections through Split of forecast for 00 UTC 2nd February 2007. Left pannels show wind speed (shaded) and direction (vectors) and potential temperature (white isolines). Right pannels show TKE (shaded), wind direction (vectors), vertical velocity omega in Pa/s (white lines, full lines are positive, dashed lines for negative values, isolines are plotted for values -20, -10, -5, 5, 10 and 20 Pa/s) and potential vorticity (black lines, full lines are positive, dashed lines for negative values, isolines are plotted for values -12, -8, -4, 4, 8 and 12). x-axis labels refer to the latitude, the longitude simultaneously changes as written below the x axis. The terrain height is plotted as a gray surface from the bottom, the names of the town with measuring station on the coast as well as names of mountains are also shown.

The full ALADIN model run is performed on 37 levels in the vertical but on the same horizontal grid as the operational dynamical adaptation. Two sets of experiments were performed, the non-hydrostatic (NH) and hydrostatic (HY) runs. Both use a new version of the ALADIN model with the new cloud and precipitation parametrization scheme (GERARD et al., 2009). The high-resolution experiments are run without DFI to avoid removal of the high-frequency wave energy from the initial conditions (TERMONIA, 2008) that also affects fast meteorological waves. Special care was taken so that horizontal diffusion does not remove the meteorologically impotant high frequency waves from the model simulation. Although the usage of SLHD reduces the intensity of NHD, the intensity of NHD was further diminished via dedicated tuning parameter, allowing short high amplitude waves to develop downstream of the mountains. Model was used with the complete physical parametrization set.

4 Model results

The NH model simulation for 00 UTC on 2nd February 2007 shows variability in 10 m wind direction and strength (Figure 8) that is mostly controlled by the terrain configuration (Figure 1). Downslope windstorms developed on Dinara and Biokovo mountains. Upwind (northeast) of Dinara, Svilaja and Biokovo mountains, surface wind is in the opposite direction than the wind above. There are several possible reasons for this. As the wind approaches the obstacle, it turns towards lower pressure. Surface wind could be reversed due to downslope breeze developed during the night and decoupled from the synoptic scale winds by a temperature inversion, or upstream blocking if the wind speed is not sufficient for the air to ascend the mountain ridge in the stable atmosphere. Another reason could be the occurence of atmospheric rotors in the valley between the mountains.

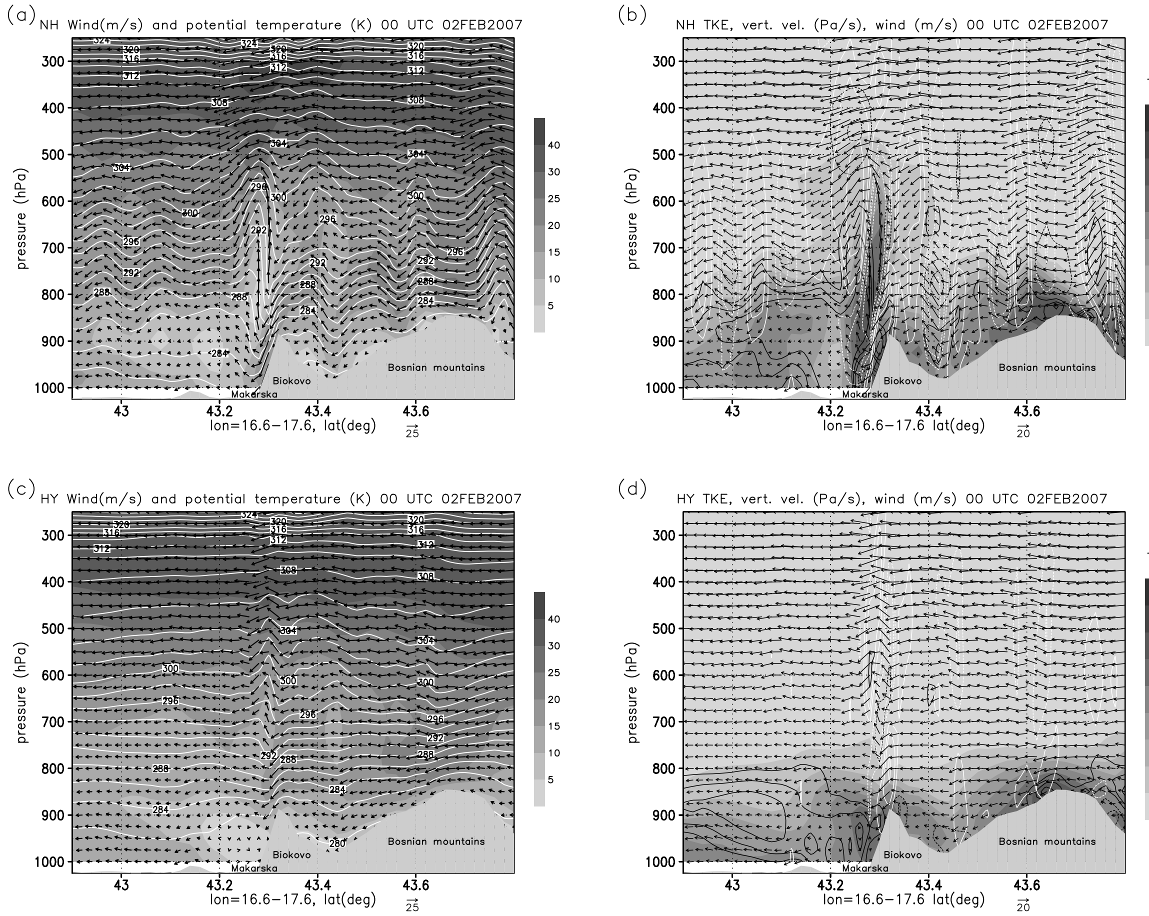

Figure 10: As Figure 9 but for Makarska.

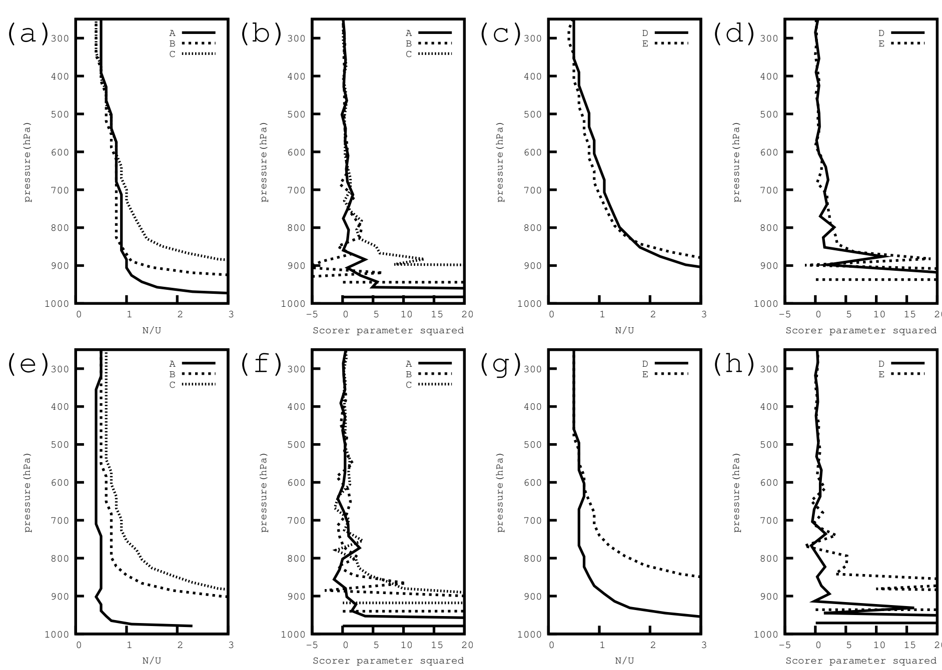

Figure 11: Brunt Vaisala frequency divided by wind speed multiplied by 1000 (pannels a, c, e and g) and Scorer parameter multiplied by 10^6 (pannels b, d, f and h) for the points A, B and C along Split (pannels a, b, e and f) and D and E along Makarska (pannels c, d, g and h) cross sections for 00 UTC 2[nd] (pannels a, b, c and d) and 18 UTC 3[rd] February 2007 (pannels e, f, g and h).

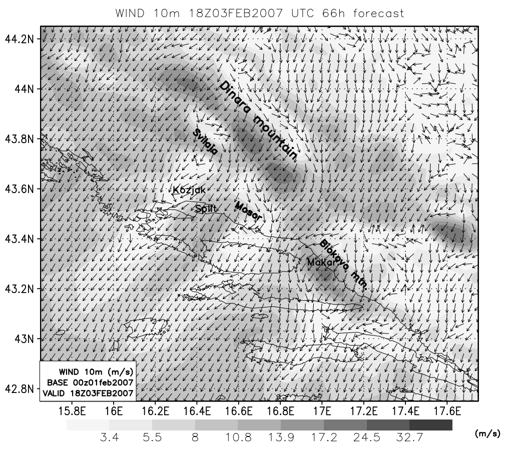

Figure 12: As Figure 8 but for 18 UTC 3rd February 2007.

Vertical cross-sections are obtained by vertical interpolation of model fields from model levels to isobaric surfaces and then horizontal interpolation to the point on the cross-section. This procedure was necessary to obtain the graphical representation but it might have removed some high resolution features from the model results.

The Split cross-section of wind vectors that represent the component of horizontal wind parallel to the cross section and vertical wind component and potential temperature obtained with NH run (Figure 9a) shows trapped wave over Dinara mountain. The wave spreads up to 500 hPa where it diminishes in a less stable layer. Between 700 and 500 hPa, the cross-mountain airflow is weaker and the isentropes and the wind vectors are almost vertical and associated with local TKE maximum (Figure 9b) as well as negative PV (black isolines in Figure 9b). Bellow 700 hPa, there are trailing waves downstream of Bosnian mountains and Dinara mountain. Downslope wind on Dinara mountain is enhanced by reflection of the wave energy from the more turbulent layer above, but only slightly enhanced at Split. Below the crests of the trailing waves, the air flow is slow, TKE and PV are high and some arrows even show the opposite wind direction, though the opposite wind direction is more evident in the 10 m wind (Figure 8). Above 700 hPa, the wave energy is more concentrated above Dinara. Atmosphere is more stable in the layer between 850 and 500 hPa than the tropospheric layers below and above. Trailing waves diminish downstream as the lower portion of the atmosphere becomes less stable further from the mountain (JIANG et al., 2006). Hydrostatic model run (HY) yields only the vertically propagating waves above ridges (Figure 9c) and far less turbulence in the middle troposphere and less variability in vertical velocity (Figure 9d). Large TKE values above the sea, downstream of Split, are a consequence of less stable boundary layer in HY than in NH run.

The predicted wind speed is compared to the measured values for the entire 72 hour forecast period in Figure 3. The ten minute measurements of the wind speed 10 meters above ground are shown in full line, the 72 hour forecast run starting from 00 UTC 1st February 2007 in 8 km resolution is shown with the dashed line, 2 km resolution full run with hydrostatic dynamics is shown in dot dash line, and non-hydrostatic run is shown in dotted line.

Between Dinara mountain and Split, there is a wide valley with a narrow gap opening in the direction towards Split. This gap is not resolved in 2 km resolution. Valley wind and the land-sea breeze that usually develops during the night could lead to a strong gap wind, expected to be strongest at the exit from the gap and enhanced by the pressure gradient across the coastal mountains that usually acompanies bura episodes. Another mechanism for the short episodes of strong bura during the night could be cold air avalanches (WHITEMAN, 2000) that may happen several times during one night as a consequence of cold air pooling in the valley upstream of Split. WHITEMAN et al. (2009) described the development of a shallow temperature deficit layer after the sunset that frees the upper level wind from the frictional deceleration. The increased vertical shear causes mixing, temperature variations and momentum exchange. This could explain the rapid changes in the measured temperature, wind and pressure, but the wind speeds described in WHITEMAN et al. (2009) were in the range of 2-4 m/s, not comparable with the measurements to these bura cases. Finally, the unpredicted bura could be consequence of exchange in the regime between the downslope windstorm and trapped lee waves and associated rotors that developed downstream of Dinara mountain. In Makarska, strong wind episodes (Figure 3b) are associated with northeast direction (Figure 4b) while moderate wind is associated with other, predominately southwest direction. In Split, the northeast wind direction prevailed during the evening on 1st and on the 2nd February and the southwest wind was not recorded in the same period, but only before both bura episodes, around 12 UTC on 1st and 3rd February. There is little evidence of rotors in the vertical cross sections, but the 10 m wind output of the NH model simulations downstream of both Dinara and Svilaja mountains, northwest from Split and on the coast southeast of Makarska does show reversals in the wind direction. The comparison of modelled and measured vertical profiles for Zagreb (Figure 6a) and Zadar (Figure 6b) reveal that neither HY nor NH run simulated the existence of the temperature inversion that were measured at 850 and 600 hPa. The one at 850 hPa is close to the top of the Dinara mountain ridge and in combination with increasing cross-barrier flow with height, favours development of trapped lee waves and rotors (VOSPER, 2004).

Figure 11 shows vertical profiles of Na/U for a=1000 m and Scorer parameter $l^2 = \frac{N^2}{U^2} - \frac{1}{U}\frac{\partial^2 U}{\partial z^2}$ multiplied

by 10^6 (corresponding to l^2a^2 for a=1000 m) for three points along the Split vertical profile and two points along the Makarska vertical profile. The scaling mountain halfwidth a is the same for all points. The halfwidths of Dinara and Biokovo mountains is about 5 km while the height of both ridges is about 1.5 km. On the Split profile, point "A" (16.7,43,7°) is just upstream of Split, point "B" (16.9,43.8°) is upstream of Dinara and point "C" (17.4,44.2°) is upstream of Bosnian mountains. On the Makarska profile, point "D" (17.2,43.4°) is upstream of Biokovo and point "E" (17.6,43.8°) is upstream of the Bosnian mountains. When the wind shear contribution is large, the Scorer paramerer l^2a^2 decreases faster than Na/U (Figure 11).
NH run predicted stronger 10 m wind for Makarska location than the HY run. The wind storm in Makarska develops too early and is too strong. This is associated with strong signal in modelled pressure (Figure 5b) since NH run also exaggerated pressure variations. It is possible to attribute this to two possible sources. One is a too weak horizontal diffusion in the model. The runs with increased SLHD intensity have removed this feature from the pressure field, but the downslope windstorm did not reach the sea level. Another reason could be the absence of the DFI in the initialization. It was not used since it removes high frequency non-meteorological waves, but unfortunately also the fast moving high frequency meteorological waves (TERMONIA, 2008). The scale-selective DFI that leaves the fast short meteorological waves was not available for this study.
The NH model run develops deep critical layer of overturning streamlines with reversal of the cross-mountain flow, vertical isentropes (Figure 10a) and large TKE values (Figure 10b) in the stable layer from 850 to 600 hPa. There is also a lot of wave activity in the same layer, both upstream and downstream of the Biokovo mountain (Figure 10a). Large vertical velocity variations in the lee of the Biokovo mountain correspond to the hydraulic jump, and large PV values (Figure 10b) are related to the cyclonic vortex visible in 10 m wind close to Makarska (Figure 8). The wave activity diminishes in the less stable layers above and below. The HY run produced vertically propagating wave above Biokovo mountain, little wave activity due to other mountain ridges upstream and no waves downstream (Figure 10c) with lower TKE values (Figure 10d). The N/U and Scorer parameters have similar profiles in D and E points (Figure 11 c and d).

In the case of 3rd February 2007, the cross-barrier wind component increases with height above Bosnian mountains only up to 700 hPa. Above this layer, wind speed is even larger, but mostly parallel to the mountain range and perpendicular to the cross-section (Figure 13a). The static stability slowly increases with height. Downstream of each mountain ridge, the downslope wind component strengthens. The descending air stabilizes the atmosphere, making the air in the lower troposphere more stable downstream than upstream of the obstacle, but the wind speed increases so that the Na/U ratio decreases (Figure 11). The height of the mountain ridges and valleys decreases downstream. There are more short waves in the potential temperature field in HY than in NH run in the vertical cross-sections between Dinara and Split for the levels between 950 and 700 hPa. The apparent short-wavelength wave in the hydrostatic run is a consequence of vertically propagating hydrostatic wave with upstream tilted phase lines formed above Mosor and Svilaja mountains (see Figure 1). Those mountains are very close to this vertical cross section and the direction of the horizontal wind is not exactly perpendicular to the mountains at that height but more from north-northeast. In the non-hydrostatic run, the waves generated by Dinara mountain propagate downstream and interact with waves produced on other mountains on the way. NH run produces higher TKE values in the middle troposphere, with an exception of an area directly above Dinara ridge (Figure 13b). HY run produces more TKE there (Figure 13d) since the wave energy spreads only upward and not downstream. Boundary layer above Bosnian mountains and Adriatic sea is less stable in HY than in NH run. Consequently, TKE values are also larger. Large PV values downstream of Dinara Mountain at 500 hPa are far more pronounced in the NH run (Figure 13 b and d and Figure 14 b and d) and the southwest wind component is stronger. The Na/U and the Scorer parameter decrease with height, and the decrease happens lower in the atmosphere as the point is closer to the coastline, but the values of the parameters are higher in the first case (Figure 11 a and b) than in the second case (Figure 11 e and f) when the parameter values decrease after each ridge.
Model did not reproduce the temperature inversion measured above Zadar (Figure 7b). This temperature inversion could be responsible for the strengthening of the windstorm in Split in the late evening of 3rd February 2007 that model did not predict (Figure 3a).
The severe downslope windstorm in Makarska of late afternoon and evening on 3rd February 2007 was predicted by both HY and NH runs (Figure 3b). It was associated with a rapid decrease in pressure, that was also predicted by the model (Figure 5b), although the peak intensity in the wind speed and low pressure values were not reached by the model simulations. Values of Na/U and the Scorer parameter (Figure 11 g and h) are less than 1 above 800 hPa in point "B" and above 900 hPa in point "A" upstream of Biokovo mountain. The nonlinear effects of overturning streamlines, reversed flow, wave breaking and large TKE values are important in both runs. The overturning streamlines and flow reversal are stronger in the HY run downstream of Bosnian mountains (Figure 14c) but TKE production is more intensive in the NH run (Figure 14b).

5 Summary and conclusions

Operational forecast in CMHS uses ALADIN model for a 2 km resolution dynamical adaptation procedure that

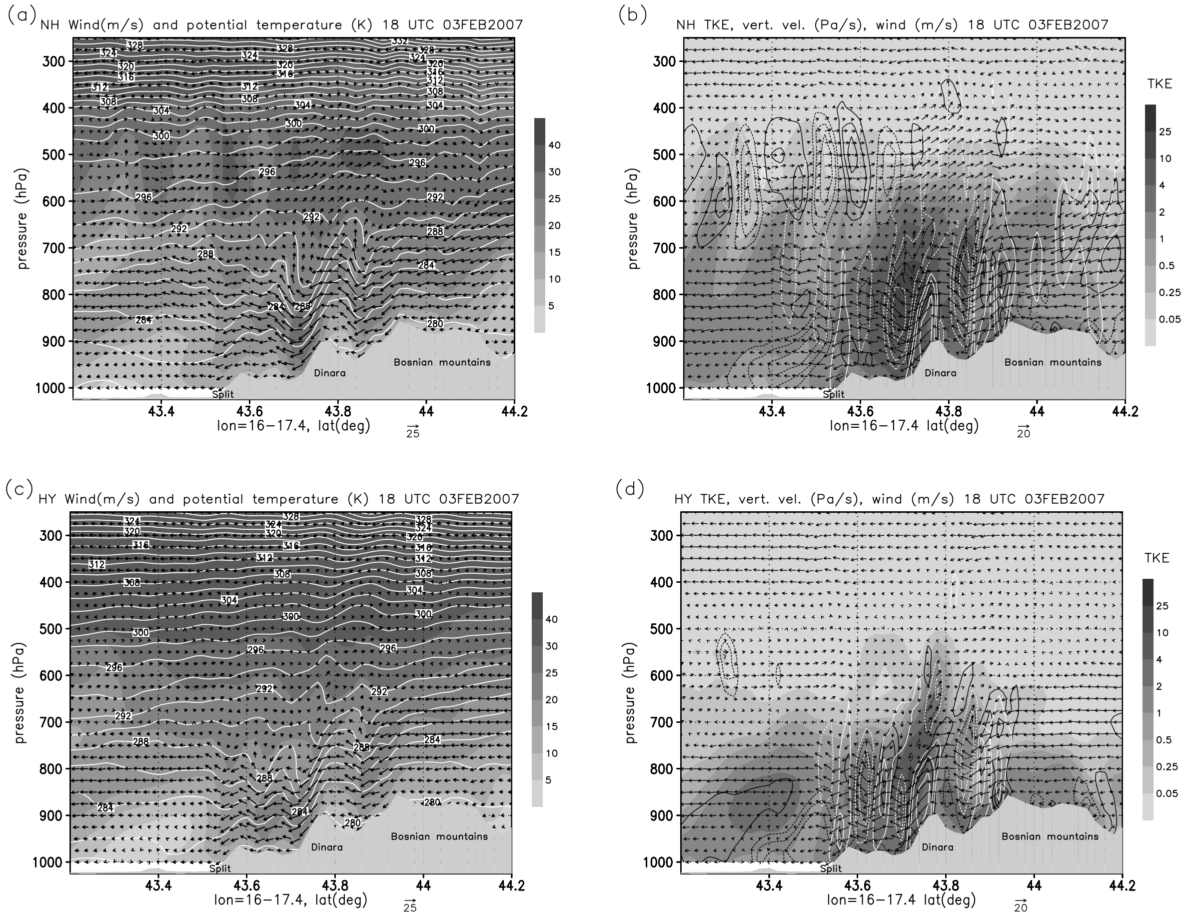

Figure 13: As Figure 9 but for 18 UTC 3rd February 2007.

provides high resolution forecast of 10 m wind. It was found reliable for bura cases by previous studies, although the model uses hydrostatic dynamics, crude vertical resolution above the surface layer and only turbulence parametrization.

The two cases of strong and severe bura that were not predicted by the operational forecast occured in the night from 1st to 2nd February 2007 and in the late afternoon and evening on 3rd February. The cases were analyzed using wind and pressure measurements from two automatic stations situated in locations hit by these bura episodes and ALADIN model runs in high resolution. Vertical soundings were used from both Croatian stations where this measurements are done. These are relatively far from the area hit by bura episode, but are the closest available to estimate the quality of the modelled vertical structure of the atmosphere and allow insight into the real vertical profiles.

The full 72 hour ALADIN forecast was run on 2 km resolution on 37 levels using the complete set of physics parameterizations. Two sets of experiments were done, using hydrostatic and nonhydrostatic dynamics. Only the least diffusive set-up of horizontal diffusion scheme is shown here. The problem of horizontal diffusion in high resolution is beyond the subject of this case study so it is not described here in more detail. Non-hydrostatic effects become more important for narrow mountains. This can be seen in the model results since the largest differences between the hydrostatic and nonhydrostatic model forecast can be observed for Makarska for the first bura case but almost none in the second case.

The vertical profiles of Na/U and l^2 (Figure 11) show that both parameters have higher values in point D (upstream Dinara) and lower values in point E (upstream Bosnian mountains) for the 1st case (Figure 11 c and d) than for the 2nd case (Figure 11 g and h). Therefore, in the first case Bosnian mountains generated lee waves that increased turbulence above Biokovo. This turbulent region served as a critical level that reflected the wave energy and enhanced the downslope windstorm. In the second case, the environmental flow reversed direction above Biokovo mountain so the downslope windstorm developed in both HY and NH model runs. Both parameters have higher values for the 1st case (Figure 11 a and b) than in the 2nd one (Figure 11 e and f) for the A, B and C profiles upstream of Split. The waves that trail behind Dinara are obvious in the 1st case (Figure 9a) and the downslope windstorm on Dinara is stronger in the

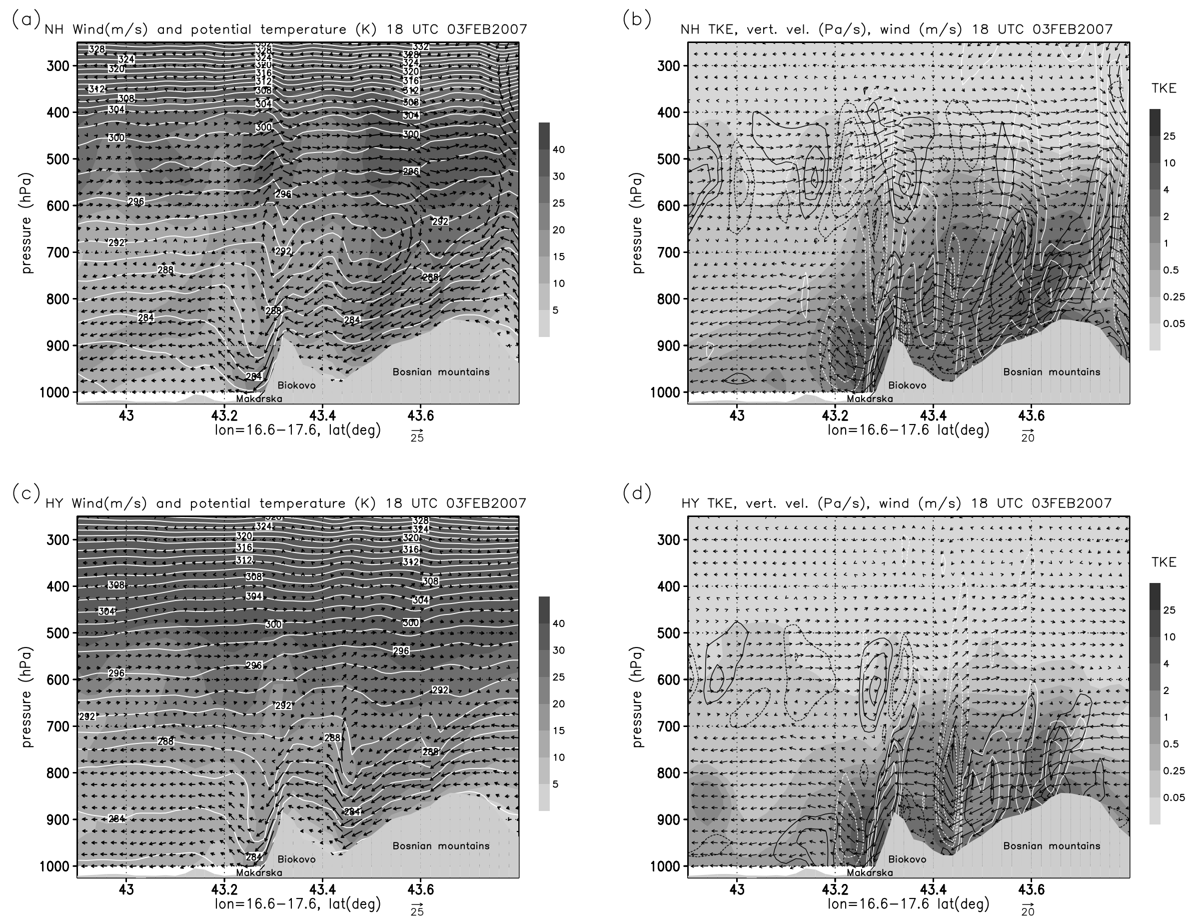

Figure 14: As Figure 10 but for 18 UTC 3rd February 2007.

NH run for the both cases, but in the model simulation the jet does not reach down to the sea level.

Although the NH model did predict the short episode of strong bura in Split during the first bura case, the peak was too early in the afternoon, and the predicted wind speed reached lowest values when the measured ones are the highest. Obviously, one could say that the vertical structure of the atmosphere was not predicted well since it misses the near mountain-top temperature inversion. The formation of rotors and low-level turbulent zones is favoured when an inversion resides just above the mountain top level (VOSPER, 2004). A deep and stable layer with horizontal wind speed that increases with height above the mountain leads to trapped lee waves. Rapid changes in wind speed could be the consequence of the rapid rotor evolution and shifting of the wavelength or amplitude of the mountain waves above. In that situation individual rotors would form and advect downstream before dissipating, but the measured wind direction and model simulations do not support this theory, at least for Split. On the other hand, the same model run overpredicted wind speed for Makarska in the first bura case, as a consequence of too strong variations in pressure.

Finally, the second case of bura was predicted well for the same location by both hydrostatic and nonhydrostatic model runs although it was far in the forecast range (66 hrs). This confirms that even these short lived bura events are predictable if the environmental conditions that lead to bura development such as self induced or environmental critical levels, are modelled correctly. Unfortunately, the 850 hPa level temperature inversion measured above Zadar is missing in the model runs for the first case. The inversion and associated environmental critical level would enhance the downslope windstorm. The possibility of perturbing upstream conditions in the model so that the temperature inversion is introduced remains a subject for further research.

Acknowledgments

The authors wish to thank Ivana STIPERSKI for advice, literature and for being the patient listener. The authors thank the Croatian Ministry of Science who supported this research through Grant 004-1193086-3036 to the Croatian Meteorological and Hydrological Service. The manuscript has benefited from the comments of the two anonymous reviewers as well as Hans VOLKERT who suggested several improvements.

References

Bajić, A., S. Ivatek-Šahdan, K. Horvath, 2007: Spatial distribution of wind speed in Croatia obtained using the ALADIN model. – Cro. Meteor. J. **42**, 67–77.

Branković, Č., B. Matjačić, S. Ivatek-Šahdan, R. Buizza, 2007: Dynamical downscaling of ECMWF EPS forecasts applied to cases of severe weather in Croatia – ECMWF RD Technical Memorandum 507, 38 pp. Available from ECMWF, Shinfield Park, Reading, RG2 9AX, UK.

Branković, Č., B. Matjačić, S. Ivatek-Šahdan, R. Buizza, 2008: Downscaling of ECMWF Ensemble Forecasts for Cases of Severe Weather: Ensemble Statistics and Cluster Analysis. – Mon. Wea. Rev. **136**, 3323–3342.

Brzović, N., 1998/1999a: A case study of a cold air outbreak on 20 April 1997 over Croatia. – Cro. Meteor. J. **33/34**, 1–18.

Brzović, N., 1999b: Factors affecting the Adriatic cyclone and associated windstorms. – Contrib. Atmos. Phys. **72**, 51–65.

Brzović, N., V. Jurčec, 1997: Numerical simulation of the Adriatic cyclone development. – Geofizika **14**, 29–46.

Catry, B., J.-F. Geleyn, M. Tudor, P. Bénard, A. Trojáková, 2007: Flux-conservative thermodynamic equations in a mass-weighted framework. – Tellus **59A**, 71–79.

Clark, T. L., W. R. Peltier, 1977: On the Evolution and Stability of Finite-Amplitude Mountain Waves. – J. Atmos. Sci. **34**, 1715–1730.

Durran, D. R., 1986a: Another Look at Downslope Windstorms. Part I: The Development of Analogs to Supercritical Flow in an Infinitely Deep, Continuosly Stratified Fluid. – J. Atmos. Sci. **43**, 2527–2543.

Durran, D.R., 1986b: Mesoscale meteorology and forecasting. – In: Ray, P.S. (Ed.), Mountain waves, Amer. Meteor. Soc., 472–492.

Enger, L., B. Grisogono, 1998: The response of bora-type flow to sea surface temperature. – Quart. J. Roy. Met. Soc. **124**, 1227–1244.

Geleyn, J.-F., F. Váňa, J. Cedilnik, M. Tudor, B. Catry, 2006: An intermediate solution between diagnostic exchange coefficients and prognostic TKE methods for vertical turbulent transport. – In: Coté J. (Ed.), WMO-CAS/JSC Working Group on Numerical Experimentation Blue Book. Report No. 36, WMO, 4.11–4.12.

Geleyn, J.-F., B. Catry, Y. Bouteloup, R. Brožková, 2008: A statistical approach for sedimentation inside a microphysical precipitation scheme. – Tellus **60A**, 649–662.

Gerard, L., J.-M. Piriou, R. Brožková, J.-F. Geleyn, D. Banciu, 2009: Cloud and precipitation parametrization in a meso-gamma scale operational weather prediction model. – Mon. Wea. Rev. **137**, 3960–3977.

Grisogono, B., D. Belušić, 2009: A review of recent advances in understanding the meso- and microscale properties of the severe Bora wind. – Tellus **61A**, 1–16.

Grubišić, V., I. Stiperski, 2009: Lee-Wave Resonances over Double Bell-Shaped Obstacles. – J. Atmos. Sci. **66**, 1205–1228.

Hertenstein, R. F., 2009: The Influence of Inversions on Rotors. – Mon. Wea. Rev. **137**, 433–446.

Hertenstein, R. F., J. P. Kuettner, 2005: Rotor types associated with steep lee topography: influence of the wind profile. – Tellus **57A**, 117–135.

Horvath, K., S. Ivatek-Šahdan, B. Ivančan-Picek, V. Grubišić, 2009: Evolution and Structure of Two Severe Cyclonic Bora Events: Contrast between the Northern and Southern Adriatic. – Weather and forecasting **24**, 946–964.

Ivatek-Šahdan, S., B. Ivančan-Picek, 2006: Effects of different initial and boundary conditions in ALADIN/HR simulations during MAP IOPs. – Meteorol. Z. **15**, 187–197.

Ivatek-Šahdan, S., M. Tudor, 2004: Use of high-resolution dynamical adaptation in operational suite and research impact studies. – Meteorol. Z. **13**, 99–108.

Jiang, Q., J.D. Doyle, R.B. Smith, 2006: Interaction between Trapped Waves and Boundary Layers. – J. Atmos. Sci. **63**, 617–633.

Jurčec, V., N. Brzović, 1995: The Adriatic bora: special case studies. – Geofizika **12**, 15–32.

Keller, T.L., 1994: Implications of the Hydrostatic Assumption on Atmospheric Gravity Waves. – J. Atmos. Sci. **51**, 1915–1929.

Klemp, J.B., D.R. Durran, 1987: Numerical Modelling of Bora Winds. – Meteor. Atmos. Phys. **36**, 215–227.

Laprise, R., W.R. Peltier, 1989a: On the Structural Characteristics of Steady Finite-Amplitude Mountain Waves over Bell-Shaped Topography. – J. Atmos. Sci. **46**, 586–595.

—, —, 1989b: The Linear Stability of Nonlinear Mountain Waves: Implications for the Understanding of Severe Downslope Windstorms. – J. Atmos. Sci. **46**, 545–564.

—, —, 1989c: The Structure and Energetics of Transient Eddies in a Numerical Simulation of Breaking Mountain Waves. – J. Atmos. Sci. **46**, 565–585.

Louis, J.-F., M. Tiedtke, J.-F. Geleyn, 1982: A short history of PBL parameterization at ECMWF. – In: Proceedings from the ECMWF Workshop on Planetary Boundary Layer Parameterization, 25-27 November 1981, ECMWF, 59–79.

Lynch, P., X.-Y. Huang, 1994: Diabatic Initialization using recursive filters. – Tellus **46A**, 583–597.

Machenhauer, B., J.E. Haugen, 1987: Test of a spectral limited area shallow water model with time-dependent lateral boundary conditions and combined normal mode/semi-lagrangian time integration schemes. – In: Proceedings from the ECMWF Workshop on Techniques for Horizontal Discretization in Numerical Weather Prediction Models, 2–4 November 1987, ECMWF, 361–377.

Nance, L.B., D.R. Durran, 1997: A Modeling Study of Nonstationary Trapped Mountain Lee Waves. Part I: Mean-Flow Variability. – J. Atmos. Sci. **54**, 2275–2291.

—, —, 1998: A Modeling Study of Nonstationary Trapped Mountain Lee Waves. Part II: Nonlinearity. – J. Atmos. Sci. **55**, 1429–1445.

Peltier, W.R., T.L. Clark, 1979: The Evolution and Stability of Finite-Amplitude Mountain Waves. Part II: Surface Wave Drag and Severe Downslope Windstorms. – J. Atmos. Sci. **36**, 1498–1529.

Queney, P., 1948: The problem of air flow over mountains: A summary of theoretical studies. – Bull. Amer. Meteor. Soc. **29**, 16–26.

Ralph, F.M., P.J. Neiman, T. L. Keller, D. Levinson, L. Fedor, 1997: Observations, Simulations, and Analysis of Nonstationary Trapped Lee Waves. – J. Atmos. Sci. **54**, 1308–1333.

REDELSPERGER, J.L., F. MAHÉ, P. CARLOTTI, 2001: A Simple And General Subgrid Model Suitable Both For Surface Layer And Free-Stream Turbulence. – Bound.-Layer Meteor. **101**, 375–408.

REINECKE, P.A., D.R. DURRAN, 2009: Initial-Condition Sensitivities and the Predictability of Downslope Winds. – J. Atmos. Sci. **66**, 3401–3418.

SIMMONS, A.J., D.M. BURRIDGE, 1981: An Energy and Angular-Momentum Conserving Vertical Finite-Difference Scheme and Hybrid Vertical Coordinates. – Mon. Wea. Rev. **109**, 758–766.

SMITH, R.B., 1979: The influence of mountains on the atmosphere. – Adv. Geophys. **21,** 87–230.

—, 1985: On Severe Downslope Winds. – J. Atmos. Sci. **42**, 2597–2603.

—, 1987: Aerial Observations of the Yugoslavian Bora. – J. Atmos. Sci. **44**, 269–297.

TERMONIA, P., 2008: Scale-Selective Digital-Filtering Initialization. – Mon. Wea. Rev. **136**, 5246–5255.

TUDOR, M., S. IVATEK-ŠAHDAN, 2002: MAP IOP 15 Case Study. – Cro. Meteor. J. **37**, 1–14.

VÁŇA, F., P. BÉNARD, J.-F. GELEYN, A. SIMON, Y. SEITY, 2008: Semi-Lagrangian advection scheme with controlled damping: An alternative to nonlinear horizontal diffusion in a numerical weather prediction model. – Quart. J. Roy. Meteor. Soc. **134**, 523–537.

VOSPER, S.B., 2004: Inversion effects on mountain lee waves. – Quart. J. R. Meteor. Soc. **130**, 1723–1748.

WANG, T.-A., Y.-L. LIN, 2000: Effects of shear and sharp gradients in static stability on two-dimensional flow over an isolated mountain ridge. – Meteor. Atmos. Phys. **75**, 69–99.

WHITEMAN, C.D., 2000: Mountain Meteorology: Fundamentals and Applications – Oxford University Press, pp. 355.

WHITEMAN, C.D., S.W. HOCH, G.S. POULOS, 2009: Evening Temperature Rises on Valley Floors and Slopes: Their Causes and Their Relationship to the Thermally Driven Wind System. – J. Appl. Meteor. Climatol. **48**, 776–788.

ŽAGAR, M., J. RAKOVEC, 1999: Small-scale surfae wind prediciton using dynamical adaptation. – Tellus **51A**, 489–504.